

<https://doi.org/10.15407/ujpe67.10.707>

V.O. ZHELTONOZHSKY, D.E. MYZNIKOV, A.M. SAVRASOV, V.I. SLISENKO

Institute for Nuclear Research, Nat. Acad. of Sci. of Ukraine  
(47, Nauky Ave., Kyiv 03028, Ukraine; e-mail: [asavrasov@kinr.kiev.ua](mailto:asavrasov@kinr.kiev.ua))

## DETERMINATION OF $^{59}\text{Ni}$ AND $^{55}\text{Fe}$ CONTENTS IN NPP STRUCTURAL ELEMENTS

---

*The structural materials from the 2nd unit of the Chornobyl NPP were irradiated by bremsstrahlung photons with an end-point energy of 37 MeV. From the measured  $\gamma$ -spectra, using the ratios among the  $^{57}\text{Co}$ ,  $^{54}\text{Mn}$ , and  $^{58}\text{Co}$  activities, the concentrations of  $^{58}\text{Ni}$  and  $^{56}\text{Fe}$  isotopes were determined in compare with the concentrations of  $^{59}\text{Co}$ . Using the obtained data and the measured  $^{60}\text{Co}$  activity in the studied samples, we developed a method for determining the  $^{59}\text{Ni}$  and  $^{55}\text{Fe}$  activities. Radiochemical validation of the created method was performed, and good quantitative agreement of  $^{59}\text{Ni}$  and  $^{55}\text{Fe}$  activities obtained by spectroscopic and radiochemical methods was found.*

*Keywords:* flux-weighted average yields, photoactivation method, gamma-spectrometry, nickel, ferrum.

### 1. Introduction

Currently, about 200 industrial and more than 500 research reactors have been stopped and either are decommissioned or being decommissioned. This is mainly associated with the fact that the first nuclear power plants (NPPs) were designed for a service life of 30 years. However, after the reconstruction, the service life of some of them was prolonged for another 5–10 years. Although the design service life of modern reactor installations comprises from 40 to 60 years, the issue concerning their decommissioning still remains challenging.

Decommissioning of NPPs after their expired lifetime is the necessary stage of their life cycle and supposes the implementation of a set of measures aimed at removing the nuclear fuel. During the reactor operation under neutron irradiation, its structural materials, thermal insulating shafts, and inner specific layers become activated. Furthermore, the radioactive corrosion and fission products can de-

posit onto the surface of the equipment in technological contours and blocking construction structures in premises, where this technological equipment is arranged. The total waste amount of various materials obtained when decommissioning any reactor can reach hundreds of  $\text{m}^3$ . The spent radionuclides start to disintegrate immediately after the installation has been switched off and have a wide range of half-life periods  $T_{1/2}$ .

Radioactive materials that are formed during the regular reactor exploitation have some specific properties, namely, new mass and isotopic contents of radioactive materials, which arise owing to the activation of structural and building materials; the presence of radionuclides with very long half-life periods; the presence of a substantial amount of  $\beta$ - and  $\gamma$ -ray emitters; and the presence of a huge amount of materials that can be reused after the appropriate recycling. Since the body of irradiated structural materials is huge, it is quite difficult to carry out a thorough characterization and identification of radionuclides accumulated in them making use of only radiochemical methods.

© V.O. ZHELTONOZHSKY, D.E. MYZNIKOV,  
A.M. SAVRASOV, V.I. SLISENKO, 2022

ISSN 2071-0186. Ukr. J. Phys. 2022. Vol. 67, No. 10

Besides iron, nickel is also widely used in stainless steels and alloys in the structural materials of NPPs [1, 2]. The nickel content in steels that are used in the construction materials of reactor installations is, on average, not lower than 8% of the total mass and can reach a value of 20–30%. Against the background of the total mass of structural materials of the power unit, the nickel mass can amount to dozens of tons. In the natural isotopic mixture of nickel, the content of  $^{58}\text{Ni}$  equals 68.1%. Therefore, the long-lived radioisotope  $^{59}\text{Ni}$  ( $T_{1/2} = 7.6 \times 10^4$  years) is accumulated in the steel structural materials in the course of the regular reactor exploitation. This radioisotope decays via the electron capture accompanied by the characteristic  $\gamma$ -ray emission with very low energy, which makes the determination of  $^{59}\text{Ni}$  activity in the structural materials of NPPs by means of standard gamma spectrometry methods rather a complicated task.

At the same time, if the iron isotope  $^{54}\text{Fe}$ , the content of which in the natural mixture equals 5.8%, is irradiated, the isotope  $^{55}\text{Fe}$  with  $T_{1/2} = 2.73$  years, is generated. This isotope also decays via the electron capture, but the latter is accompanied only by the characteristic radiation. Therefore, the development of non-radiochemical methods for the determination of the activity of long-lived radionuclides  $^{55}\text{Fe}$  and  $^{59}\text{Ni}$  is a challenging task, which is the aim of this work.

## 2. Experimental Technique and Results of Measurements

According to the developed procedure, we propose to determine the activities of accumulated iron and nickel radioisotopes in the structural materials of NPPs on the basis of the activity of the isotope  $^{60}\text{Co}$  with a half-life period of 5.27 years. Natural cobalt consists of only  $^{59}\text{Co}$  and is inextricably associated with nickel, because it is an impurity in nickel ores. In steels used for the NPP structural materials, the cobalt admixture should not exceed 0.5%. However, as a result of the very large cross-section of thermal neutron capture by  $^{59}\text{Co}$  nuclei, there emerges  $^{60}\text{Co}$  whose activity can be easily identified according to the presence of 1173-keV and 1333-keV  $\gamma$ -lines in the spectra of all irradiated structural materials.

Some series of calculations carried out for reactors of various types [3] showed that most of the accumulated products of the reactor activation are located

in the active zone vessel, and only a few radioisotopes give a dominant contribution to the total activity level. It was found that  $^{60}\text{Co}$  and  $^{55}\text{Fe}$  dominate the total activity within a time interval from 5 to 20 years after the reactor shutdown. On the other hand,  $^{60}\text{Co}$  dominates gamma radiation for 100 years after the shutdown. The nickel isotopes begin to dominate the total activity in about 20 years. A similar picture was also obtained for the reactor vessel walls, but with lower values for the cobalt and nickel radioisotope activities.

Hence, knowing the cobalt activity and the composition of structural materials with the cobalt admixture, it is possible to evaluate the amount of radioactive nuclides that are generated in the structural materials due to the  $(n, \gamma)$ -reaction in the course of the reactor operation.

To calculate the activities in the NPP structural materials, the following formula is used as a rule:

$$A = N_A \sigma \varphi [1 - \exp(-\lambda t_{\text{irr}})] \exp(-\lambda t_{\text{cool}}), \quad (1)$$

where  $N_A$  is the amount of corresponding atoms in the NPP structural materials,  $\sigma$  the activation cross-section by thermal neutrons,  $\varphi$  the average density of the thermal neutron flux irradiating the structural materials,  $t_{\text{irr}}$  the total duration of the irradiation, and  $t_{\text{cool}}$  the time lag between the irradiation and the measurement.

For  $t_{\text{irr}}$ , the operation time in effective day units is applied. This parameter is determined from the known values of energy generation  $E$  (MW $\times$ day). For the time  $t_{\text{cool}}$ , the values of the total reactor downtimes according to the existing load schedules of power units, which are averaged over a year, are used. In general, the flux density  $\varphi$  is measured at the main irradiated nodes. However, it is evident that significant variations of the flux magnitude are possible owing to the neutron rescattering. The situation with the masses of irradiated materials is even more complicated. For cobalt, in particular, it is often assumed that its mass should not exceed 0.5% of the total mass. There are substantial difficulties with the evaluation of cross-sections for reactions with thermal neutrons. In the reactor, there are “thermal” neutrons produced by the operating reactor, and their energy is much higher than the energy of thermal neutrons for which the  $(n, \gamma)$ -cross-sections were measured. The energies of thermal neutrons vary from

0.025 to 0.5 eV, whereas, in the reactor, those energies are about 2 eV (see the neutron spectrum for RBMK-1000 in work [4]).

All the aforesaid results in that the activities calculated according to formula (1) differ from the experimental values by 1 to 2 orders of magnitude. To solve this problem, we have developed a calculation technique for determining the activity of the examined nuclide with respect to the activity of  $^{60}\text{Co}$ . Knowing the activity of  $^{60}\text{Co}$  and the ratio of the researched materials with respect to cobalt impurities, it is possible to calculate the activities of isotopes that are generated in the  $(n, \gamma)$ -reaction. In order to determine the ratio of various elements in the structural materials, we suggest to apply the photoactivation technique [5].

To validate the obtained data, we analyzed the elemental composition of samples taken at the 2nd unit of the Chernobyl NPP. With the help of photoactivation method, the amount of cobalt admixture in comparison with nickel and iron was measured. In the structural materials of NPPs, nickel and iron are always present together with cobalt. Therefore, in order to avoid methodical errors, relative measurements were carried out by comparing the yields of the  $\gamma$ -lines of  $^{57,58}\text{Co}$  and  $^{54}\text{Mn}$ . For this purpose, samples selected at this unit in the region of high neutron background (RHNB), as well as in other places such as the reactor vessel (Fe), pipelines, and MNZh tubes, were irradiated on a LUE-40 accelerator at the Kharkiv Institute of Physics and Technology of the National Academy of Sciences of Ukraine [6] by a beam of bremsstrahlung  $\gamma$ -quanta with an end-point energy of 37 MeV.

The  $\gamma$ -spectrum of an irradiated iron sample is shown in Fig. 1. In order to determine the nickel/cobalt and iron/cobalt mass ratios, the corresponding intensity ratios were measured for the  $\gamma$ -lines with energies of  $\gamma 136$  keV ( $^{57}\text{Co}$ ,  $T_{1/2} = 272$  days),  $\gamma 811$  keV ( $^{58}\text{Co}$ ,  $T_{1/2} = 71$  days), and  $\gamma 834$  keV ( $^{54}\text{Mn}$ ,  $T_{1/2} = 312.1$  days) [7].  $^{57}\text{Co}$  is mainly generated in the  $(\gamma, n)$ - and  $(\gamma, p)$ -reactions with the  $^{58}\text{Ni}$  isotope, whereas  $^{58}\text{Co}$  mainly in the  $(\gamma, n)$ -reaction with the  $^{59}\text{Co}$  monoisotope. At the same time, the reactions  $^{56}\text{Fe}(\gamma, pn)^{54}\text{Mn}$  and  $^{55}\text{Mn}(\gamma, n)^{54}\text{Mn}$  are used for the identification of the  $^{56}\text{Fe}$  isotope. For irradiation, samples 50 mg in mass were applied.

The known formulas of activation analysis bring about the following ratios between the amounts of

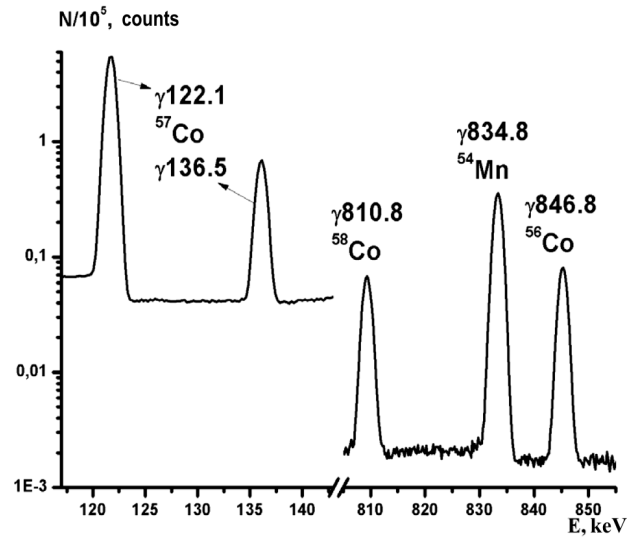


Fig. 1. Fragment of the  $\gamma$ -spectrum of activated iron (Fe) target

$^{58}\text{Ni}$  and  $^{59}\text{Co}$  atoms and between the amounts of  $^{56}\text{Fe}$  and  $^{59}\text{Co}$  ones:

$$\frac{m(\text{Ni})}{m(\text{Co})} = \frac{N(\text{Ni})(1 - e^{-\lambda(\text{Co})t_{\text{irr}}})(1 - e^{-\lambda(\text{Co})t_{\text{meas}}})}{N(\text{Co})(1 - e^{-\lambda(\text{Ni})t_{\text{irr}}})(1 - e^{-\lambda(\text{Ni})t_{\text{meas}}})} \times \frac{e^{-\lambda(\text{Co})t_{\text{cool}}}Y(\text{Co})\lambda(\text{Ni})}{e^{-\lambda(\text{Ni})t_{\text{cool}}}Y(\text{Ni})\lambda(\text{Co})}, \quad (2a)$$

$$\frac{m(\text{Fe})}{m(\text{Co})} = \frac{N(\text{Mn})(1 - e^{-\lambda(\text{Co})t_{\text{irr}}})(1 - e^{-\lambda(\text{Co})t_{\text{meas}}})}{N(\text{Co})(1 - e^{-\lambda(\text{Mn})t_{\text{irr}}})(1 - e^{-\lambda(\text{Mn})t_{\text{meas}}})} \times \frac{e^{-\lambda(\text{Co})t_{\text{cool}}}Y(\text{Co})\lambda(\text{Mn})}{e^{-\lambda(\text{Mn})t_{\text{cool}}}Y(\text{Mn})\lambda(\text{Co})}, \quad (2b)$$

where  $m(\text{Ni})$ ,  $m(\text{Co})$ ,  $m(\text{Fe})$  are the amounts of the  $^{58}\text{Ni}$ ,  $^{59}\text{Co}$ , and  $^{56}\text{Fe}$  atoms, respectively;  $\lambda(\text{Co})$ ,  $\lambda(\text{Ni})$ , and  $\lambda(\text{Mn})$  are the radioactive decay constants for  $^{58}\text{Co}$ ,  $^{57}\text{Co}$ , and  $^{54}\text{Mn}$ , respectively;  $Y(\text{Ni})$ ,  $Y(\text{Co})$ , and  $Y(\text{Mn})$  are the weighted average yields for  $^{57}\text{Co}$ ,  $^{58}\text{Co}$ , and  $^{54}\text{Mn}$ , respectively;  $N(\text{Ni})$ ,  $N(\text{Co})$ , and  $N(\text{Mn})$  are the amounts of radioactive nuclei  $^{57}\text{Co}$ ,  $^{58}\text{Co}$ , and  $^{54}\text{Mn}$ , respectively; and  $t_{\text{irr}}$ ,  $t_{\text{cool}}$ , and  $t_{\text{meas}}$  are the durations of the irradiation, cooling, and measurement stages, respectively. The presented formulas take into account that the measurements were performed a month after the irradiation, so all  $^{57}\text{Ni}$  nuclei that had been formed in the  $(\gamma, n)$ -reactions have already decayed via the electron capture by the  $^{57}\text{Co}$  nuclei.

The half-life periods  $T_{1/2}$  of the  $^{57}\text{Co}$ ,  $^{58}\text{Co}$  and  $^{54}\text{Mn}$  isotopes are equal to 271.8, 70.8, and 312.1 days, respectively [7], whereas the samples were irradiated for several hours ( $t_{\text{irr}}$ ). Hence, for the generated nuclides,  $T_{1/2} \gg t_{\text{irr}}$ . As a result, the exponential functions  $e^{-\lambda t_{\text{irr}}}$  can be expanded in the corresponding Taylor series to obtain that  $1 - e^{-\lambda(\text{Co})t_{\text{irr}}} \approx \lambda(\text{Co})t_{\text{irr}}$ ,  $1 - e^{-\lambda(\text{Ni})t_{\text{irr}}} \approx \lambda(\text{Ni})t_{\text{irr}}$ , and  $1 - e^{-\lambda(\text{Mn})t_{\text{irr}}} \approx \lambda(\text{Mn})t_{\text{irr}}$ . Since  $T_{1/2} \gg t_{\text{meas}}$  too, analogous approximations are also applicable to the exponential functions  $e^{-\lambda t_{\text{meas}}}$ :  $1 - e^{-\lambda(\text{Co})t_{\text{meas}}} \approx \lambda(\text{Co})t_{\text{meas}}$ ,  $1 - e^{-\lambda(\text{Ni})t_{\text{meas}}} \approx \lambda(\text{Ni})t_{\text{meas}}$ , and  $1 - e^{-\lambda(\text{Mn})t_{\text{meas}}} \approx \lambda(\text{Mn})t_{\text{meas}}$ . Then, Eqs. (2) read

$$\frac{m(\text{Ni})}{m(\text{Co})} \approx \frac{N(\text{Ni})\lambda(\text{Co})e^{-\lambda(\text{Co})t_{\text{cool}}}Y(\text{Co})}{N(\text{Co})\lambda(\text{Ni})e^{-\lambda(\text{Ni})t_{\text{cool}}}Y(\text{Ni})}, \quad (3a)$$

$$\frac{m(\text{Fe})}{m(\text{Co})} \approx \frac{N(\text{Mn})\lambda(\text{Co})e^{-\lambda(\text{Co})t_{\text{cool}}}Y(\text{Co})}{N(\text{Co})\lambda(\text{Mn})e^{-\lambda(\text{Mn})t_{\text{cool}}}Y(\text{Mn})}. \quad (3b)$$

Thus, for NPPs operating in the normal regime, the expressions for the  $^{55}\text{Fe}$  and  $^{59}\text{Ni}$  activity yields with regard for the quantum yields of 100% for the 834.8-keV  $\gamma$ -line ( $^{54}\text{Mn}$ ), 10.68% for the 136-keV  $\gamma$ -line ( $^{57}\text{Co}$ ), and 99.45% for the 811-keV  $\gamma$ -line ( $^{58}\text{Co}$ ) become substantially simpler and look like

$$\frac{m(\text{Ni})}{m(\text{Co})} = 9.3 \frac{N_{\gamma}(136 \text{ keV})\lambda(\text{Co})e^{-\lambda(\text{Co})t_{\text{cool}}}Y(\text{Co})}{N_{\gamma}(811 \text{ keV})\lambda(\text{Ni})e^{-\lambda(\text{Ni})t_{\text{cool}}}Y(\text{Ni})}, \quad (4a)$$

$$\frac{m(\text{Fe})}{m(\text{Co})} = 9.4 \frac{N_{\gamma}(136 \text{ keV})\lambda(\text{Co})e^{-\lambda(\text{Co})t_{\text{cool}}}Y(\text{Co})}{N_{\gamma}(835 \text{ keV})\lambda(\text{Mn})e^{-\lambda(\text{Mn})t_{\text{cool}}}Y(\text{Mn})}, \quad (4b)$$

where the coefficients 9.3 and 9.4 are the values of the quantum yield ratios between the 811-keV and 136-keV  $\gamma$ -lines and between the 835-keV and 136-keV  $\gamma$ -lines, respectively;  $N_{\gamma}(136 \text{ keV})$  is the number of counts in the peak with an energy of 136 keV accounting for the efficiency of the spectrometer registration (18.4% in this case);  $N_{\gamma}(811 \text{ keV})$  is the number of counts in the total absorption peak at an energy of 811 keV with regard for the efficiency of the spectrometer registration (5.2% in this case); and  $N_{\gamma}(835 \text{ keV})$  is the number of counts in the 835-keV peak taking the efficiency of the spectrometer registration into account (5% in this case). Since the targets are thin, the self-absorption of those  $\gamma$ -quanta can be neglected.

As was discussed in Introduction, stainless steel in the structural materials contains, as a rule, 70% of Fe, 10% of Ni, and no more than 0.5% of Co. From those data, we can estimate that the activity of  $^{55}\text{Fe}$  does not exceed  $0.5 \times A(^{60}\text{Co})$ , and the activity of  $^{59}\text{Ni}$  is lower than  $10^{-2} \times A(^{60}\text{Co})$  at the normal NPP operation. Naturally, in such materials as surfacings and thermal insulators, various activity reflection shields can considerably vary, so it is necessary to perform experimental studies of the cobalt-nickel-iron ratio with the help of photoactivation analysis. In such studies, critical are the yields of the relevant reactions.

The weighted average yield of the reaction  $^{58}\text{Ni}(\gamma, n)^{57}\text{Ni}$  was determined as a result of the convolution with an increment of 1 MeV according to the formula

$$Y = \frac{\sum_{i=1}^N \sigma_i \varphi_i}{\sum_{i=1}^N \varphi_i}, \quad (5)$$

where  $\sigma_i$  are the tabulated cross-section values for the  $^{58}\text{Ni}(\gamma, n)^{57}\text{Ni}$  reaction with monochromatic  $\gamma$ -quanta, and  $\varphi_i$  are the relative values of the flux for the spectrum of bremsstrahlung  $\gamma$ -quanta simulated in Geant4 [8] for various event numbers, which are reduced to the end-point energy value for this reaction.

To calculate the weighted average yields, the data for the reaction cross-sections were taken from two sources: the tabulated experimental data and the results calculated with the help of the Talys-1.96 program [9]. If the discrepancies between them exceeded the experimental error limits, the experimental data were used. The procedure of calculating yields for the reactions  $^{58}\text{Ni}(\gamma, n)^{57}\text{Ni}$  and  $^{59}\text{Co}(\gamma, n)^{58}\text{Co}^{\text{tot}}$  was described in detail in work [10]. When determining the amount of  $^{56}\text{Fe}$  nuclei, it is necessary to obtain the weighted average yields of the reactions  $^{56}\text{Fe}(\gamma, pn)^{54}\text{Mn}$  and  $^{55}\text{Mn}(\gamma, n)^{54}\text{Mn}$ , because the examined samples contain manganese impurities. The data for the experimental cross-sections for the former reaction are absent from the EXFOR database [11];

Table 1. Weighted average yields of analyzed reactions

Element	$^{58}\text{Ni}$ (Talys)	$^{58}\text{Ni}$ [13]	$^{59}\text{Co}$ (Talys)	$^{59}\text{Co}$ [14]	$^{55}\text{Mn}$ (Talys)	$^{55}\text{Mn}$ [12]
$Y(\gamma, n)$ , mbarn	10.1(7)	13.4(13)	24.2(17)	24.4(24)	22.0(16)	25.0(26)

therefore, they were theoretically calculated by means of the Talys-1.96 code (see Fig. 2).

For the reaction  $^{55}\text{Mn}(\gamma, n)^{54}\text{Mn}$ , the cross-section values for calculating the weighted average yield according to formula (5) were taken from the experimental work [12] (see Fig. 3).

Making use of those methods and formula (5), we calculated the weighted average yields for various elements that were contained in the irradiated samples. The obtained results are quoted in Table 1. As one can see, the difference between the experimental and theoretical results remains within the required accuracy of the method for  $^{59}\text{Co}$  and  $^{55}\text{Mn}$ , being slightly different for the reaction  $^{58}\text{Ni}(\gamma, n)^{57}\text{Ni}$ . A similar situation also takes place for the reaction  $^{58}\text{Ni}(\gamma, p)^{57}\text{Co}$ . In our research, we used the experimental data of other authors.

For the weighted average yields calculated using the data of the Talys-1.96 code, the error consists of the error obtained while simulating the bremsstrahlung spectrum in the Geant4 code, which did not exceed 7%. In the case where the experimental data were applied, the total error was somewhat higher, because the simulation error was summed up with the rms error for the experimental cross-section. For each cross-section, this error was taken into account with its weighting factor, i.e., the weighted average error was calculated. The corresponding value was found to also equal 7–8%. Therefore, the total determination error for the weighted average yields used in the subsequent calculations was within 10%.

The errors for the weighted average yields dominate in the calculation of the required ratios following formulas (4). In our case, the determination errors for the quantum yields were less than 1%, because we used the most intense  $\gamma$ -lines. The total determination error for the registration efficiency varied within an interval of 3–5% and consisted of both the determination error for the calibration source activity and the errors for the intensities and quantum yields of  $\gamma$ -lines of the calibration source. This error also included an error given by the smoothing polynomials, if the energy of a required  $\gamma$ -quantum was in between the peaks of calibration  $\gamma$ -lines. Therefore, the total error for the ratios calculated via formulas (4) was within 11–12%.

The excitation functions for the generation of the  $^{59}\text{Ni}$ ,  $^{55}\text{Fe}$ , and  $^{60}\text{Co}$  activities during the reactor op-

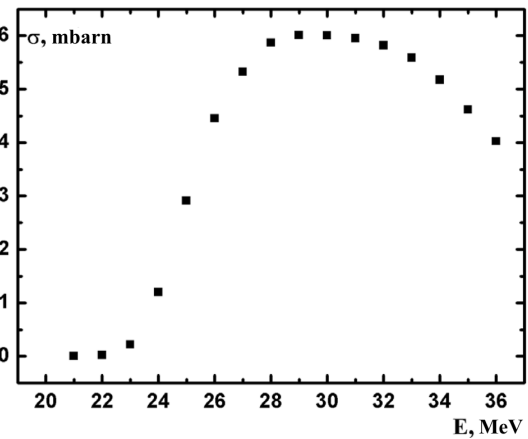


Fig. 2. Simulated excitation function for the reaction  $^{56}\text{Fe}(\gamma, pn)^{54}\text{Mn}$

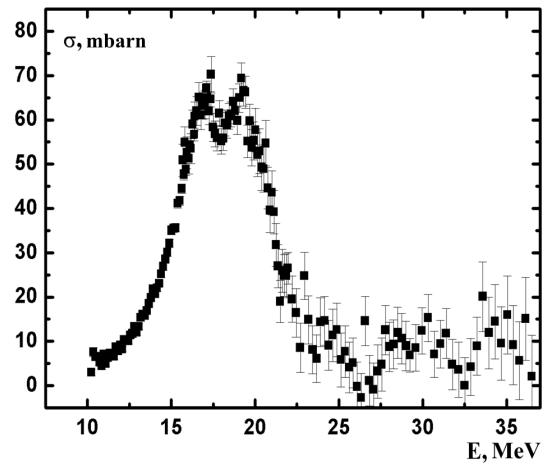


Fig. 3. Excitation function for the reaction  $^{55}\text{Mn}(\gamma, n)^{54}\text{Mn}$  from work [12]

eration are shown in Figs. 4–6, respectively. The legends at the bottom of the plots contain information about the libraries that were used for the calculation of excitation functions. The numbers of points used in the calculation are indicated in the upper right corners of the plots. The experimental measurements were carried out at energy values of 0.0253 eV, 30 keV, and 14.5 MeV. (The latter only for the reaction  $^{59}\text{Co}(n, \gamma)^{60}\text{Co}$ . In this case (see Fig. 6), the dotted curve illustrates the excitation function for the reaction  $^{59}\text{Co}(n, \gamma)^{60}\text{Co}^m$ .)

As one can see from Figs. 4–6, “thermal” neutrons provide the main contribution to the activation of cobalt, iron, and nickel. The capture cross-sections

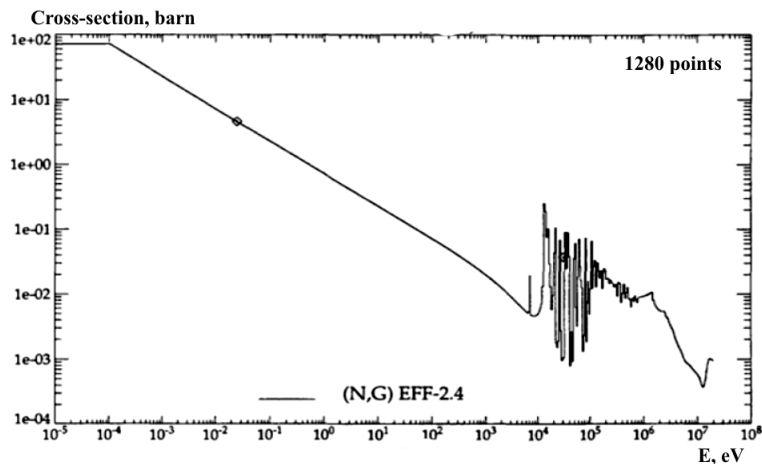


Fig. 4. Excitation function for the reaction  $^{58}\text{Ni}(n,\gamma)^{59}\text{Ni}$  [15]

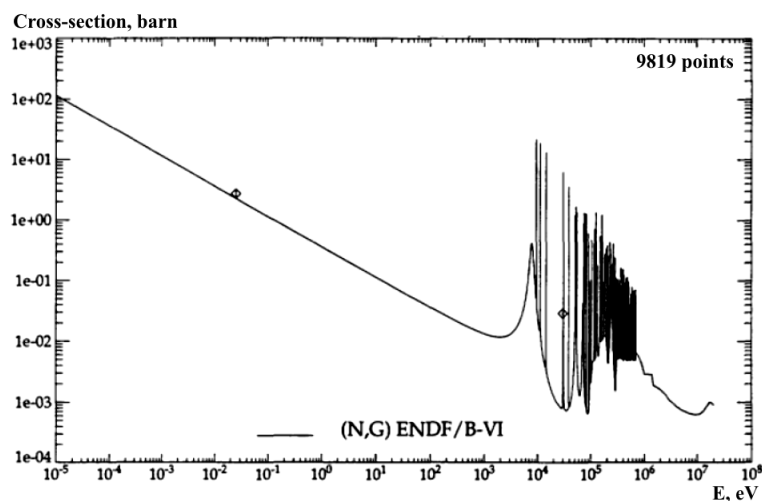


Fig. 5. Excitation function for the reaction  $^{54}\text{Fe}(n,\gamma)^{55}\text{Fe}$  [15]

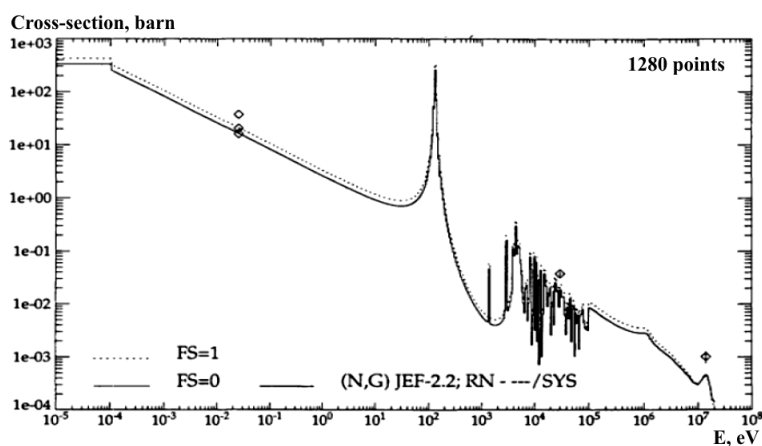


Fig. 6. Excitation function for the reaction  $^{59}\text{Co}(n,\gamma)^{60}\text{Co}$  [15]

of those neutrons are described by the formula

$$\sigma \sim \sigma(E = 0.025 \text{ eV}) \times \frac{V(E = 0.025 \text{ eV})}{V(E)},$$

where  $V(E)$  is the velocity of neutrons. One can also see that the data for a neutron energy of 0.025 eV can be used for relative measurements. The contributions from epithermal and fast neutrons can be neglected, so the tabular cross-section values just for thermal neutrons were used in further calculations. The activity ratios between the  $^{59}\text{Ni}$  and  $^{60}\text{Co}$  isotopes and between the  $^{55}\text{Fe}$  and  $^{60}\text{Co}$  ones were evaluated using the following formulas:

$$\begin{aligned} \frac{A(^{59}\text{Ni})}{A(^{60}\text{Co})} &= \\ &= \frac{(1 - e^{-\lambda(^{59}\text{Ni})t_{\text{irr}}})e^{-\lambda(^{59}\text{Ni})t_{\text{cool}}}\Phi_n\sigma_{^{58}\text{Ni}}^n N_{^{58}\text{Ni}}}{(1 - e^{-\lambda(^{60}\text{Co})t_{\text{irr}}})e^{-\lambda(^{60}\text{Co})t_{\text{cool}}}\Phi_n\sigma_{^{59}\text{Co}}^n N_{^{59}\text{Co}}} = \\ &= \frac{(1 - e^{-\lambda(^{59}\text{Ni})t_{\text{irr}}})e^{-\lambda(^{59}\text{Ni})t_{\text{cool}}}\sigma_{^{58}\text{Ni}}^n N_{^{58}\text{Ni}}}{(1 - e^{-\lambda(^{60}\text{Co})t_{\text{irr}}})e^{-\lambda(^{60}\text{Co})t_{\text{cool}}}\sigma_{^{59}\text{Co}}^n N_{^{59}\text{Co}}}, \quad (6a) \end{aligned}$$

$$\begin{aligned} \frac{A(^{55}\text{Fe})}{A(^{60}\text{Co})} &= \\ &= \frac{(1 - e^{-\lambda(^{55}\text{Fe})t_{\text{irr}}})e^{-\lambda(^{55}\text{Fe})t_{\text{cool}}}\Phi_n\sigma_{^{54}\text{Fe}}^n N_{^{54}\text{Fe}}}{(1 - e^{-\lambda(^{60}\text{Co})t_{\text{irr}}})e^{-\lambda(^{60}\text{Co})t_{\text{cool}}}\Phi_n\sigma_{^{59}\text{Co}}^n N_{^{59}\text{Co}}} = \\ &= \frac{(1 - e^{-\lambda(^{55}\text{Fe})t_{\text{irr}}})e^{-\lambda(^{55}\text{Fe})t_{\text{cool}}}\sigma_{^{54}\text{Fe}}^n N_{^{54}\text{Fe}}}{(1 - e^{-\lambda(^{60}\text{Co})t_{\text{irr}}})e^{-\lambda(^{60}\text{Co})t_{\text{cool}}}\sigma_{^{59}\text{Co}}^n N_{^{59}\text{Co}}}, \quad (6b) \end{aligned}$$

where  $A(^{59}\text{Ni})$ ,  $A(^{55}\text{Fe})$ , and  $A(^{60}\text{Co})$  are the activities of the  $^{59}\text{Ni}$ ,  $^{55}\text{Fe}$ , and  $^{60}\text{Co}$  isotopes, respectively (in Bq units);  $\Phi_n$  is the neutron flux in the reactor (in neutron/s units);  $\sigma_{^{58}\text{Ni}}^n$ ,  $\sigma_{^{54}\text{Fe}}^n$ , and  $\sigma_{^{59}\text{Co}}^n$  are the tabulated cross-section values for the reactions  $^{58}\text{Ni}(n,\gamma)^{59}\text{Ni}$ ,  $^{54}\text{Fe}(n,\gamma)^{55}\text{Fe}$ , and  $^{59}\text{Co}(n,\gamma)^{60}\text{Co}$ , respectively (in barn units); they were taken from work [7];  $\lambda(^{59}\text{Ni}) = 0.693/T_{1/2}(^{59}\text{Ni})$ ,  $\lambda(^{55}\text{Fe}) = 0.693/T_{1/2}(^{55}\text{Fe})$ , and  $\lambda(^{60}\text{Co}) = 0.693/T_{1/2}(^{60}\text{Co})$  are the radioactive decay constants for  $^{59}\text{Ni}$ ,  $^{55}\text{Fe}$ , and  $^{60}\text{Co}$ , respectively (in  $\text{s}^{-1}$  units);  $T_{1/2}(^{59}\text{Ni})$ ,  $T_{1/2}(^{55}\text{Fe})$ , and  $T_{1/2}(^{60}\text{Co})$  are the half-lives of  $^{59}\text{Ni}$ ,  $^{55}\text{Fe}$ , and  $^{60}\text{Co}$ , respectively (in s units);  $N_{^{58}\text{Ni}}/N_{^{59}\text{Co}}$  is the ratio between the amounts of  $^{58}\text{Ni}$  and  $^{59}\text{Co}$  atoms, and  $N_{^{54}\text{Fe}}/N_{^{59}\text{Co}}$  is the ratio between the amounts of  $^{54}\text{Fe}$  and  $^{59}\text{Co}$  atoms (for a given sample, formulas (6) are obtained from formulas (4) for the ratio between by the amounts of  $^{56}\text{Fe}$  and  $^{59}\text{Co}$  atoms after accounting for the content of  $^{54}\text{Fe}$  in the

Table 2. Activities of studied samples calculated by both methods

No.	$^{59}\text{Ni}$ , Bq/g		$^{55}\text{Fe}$ , Bq/g	
	Photoactivation	Radiochemical	Photoactivation	Radiochemical
1(Pipeline)	0,02(1)	<0,05	0,8(2)	<0.9
2(Tube)	0.02(1)	<0.05	0.9(2)	1.0
3(Fe, vessel)	0.02(1)	<0.05	0.6(2)	<0.6
4(RENB)	0.52(8)	0.68(15)	6.5(10)	7.1(9)

natural mixture); and  $t_{\text{irr}}$ ,  $t_{\text{cool}}$ , and  $t_{\text{meas}}$  are the duration times of irradiation, cooling, and measurement, respectively.

The activities of  $^{59}\text{Ni}$  and  $^{55}\text{Fe}$  calculated via formulas (6) are quoted in Table 2. We also calculated the activities of analyzed samples using radiochemical methods, and the results of those calculations are also presented in Table 2. As one can see, they are in a good agreement.

The total error for the activities was obtained as the square root of the summed up squared errors for the ratios whose calculation was described above, errors for the tabulated cross-sections of  $(n,\gamma)$ -reactions, and errors for the quantum yields, registration efficiencies, and peak areas of  $\gamma$ -quanta that accompany the decay of  $^{60}\text{Co}$  nuclei. The neutron flux errors were not considered, because the fluxes are absent from the formulas. The systematic error was evaluated by performing measurements on another spectrometer. It was found to be within an interval of 1–2%. In Table 2, the large magnitudes of errors of the photoactivation method, which substantially exceed 15%, stem from with a low statistical accuracy of  $\gamma$ -peaks.

### 3. Conclusions

The analysis of radionuclide yields demonstrates that when samples 10–50 mg in mass are irradiated with bremsstrahlung  $\gamma$ -quanta with an end-point energy of 37 MeV, activities sufficient for measuring the spectra of  $\gamma$ -quanta are accumulated during 3–4 h. This circumstance allows 100–200 samples to be irradiated simultaneously.

The photoactivation method for determining the activities of  $^{59}\text{Ni}$  and  $^{55}\text{Fe}$  makes it possible to significantly simplify their identification, control, and certi-

fication in steel structural materials of nuclear power plants and radioactive wastes of various types. The proposed method is more effective as compared to standard radiochemical methods owing to a large mass of irradiated structural materials and radioactive waste generated at NPPs, as well as the complexity of radiochemical methods.

The work was supported in the framework of the budget program "Support of the development of priority areas of scientific research" (KPKVK 6541230) in 2022–2023.

1. Y. Amano et al. *Design of Instrumentation and Control System for Nuclear Power Plants. Specific Safety Guide* (International Atomic Energy Agency, 2016).
2. Y. Amano et al. *Construction for Nuclear Installations. Specific Safety Guide* (International Atomic Energy Agency, 2015).
3. J.C. Evans et al. *Long-Lived Activation Products in Reactor Materials* (Pacific Northwest Laboratory, 1984).
4. E.A. Zhyrbenko, B.K. Bulkin. The main approaches to determining the activity of the structures of reactor units with VVER during their decommissioning. In: *Proceedings of the 6th International Scientific and Technical Conference "Safety Assurance of NPP with VVER"*, Podolsk, May 26–29, 2009 (OKB Gidropress, 2009), p. 1 (in Russian).
5. V.A. Zheltonozhsky, D.E. Myznikov, V.I. Slisenko, M.V. Zheltonozhskaya, A.P. Chernyaev. Determination of the long-lived  $^{10}\text{Be}$  in construction materials of nuclear power plants using photoactivation method. *J. Environ. Radioact.* **227**, 106509 (2021).
6. M.I. Aizatskiy, V.I. Beloglasov, V.N. Boriskin et al. State and prospects of the linac of nuclear-physics complex with energy of electrons up to 100 MeV. *Probl. Atom. Sci. Techn.* **91**, 60 (2014).
7. R.B. Firestone. *Table of Isotopes. 8th Edition* (Wiley Interscience, 1996).
8. S. Agostinelli et al. GEANT4 – a simulation toolkit. *Nucl. Instrum. Meth. A* **506**, 250 (2003).
9. A.J. Koning, D. Rochman. Modern nuclear data evaluation with the TALYS code system. *Nucl. Data Sheets* **113**, 2841 (2012).
10. V.O. Zheltonozhsky, D.E. Myznikov, A.M. Savrasov, V.I. Slisenko. Determination of the activity of  $^{63}\text{Ni}$  in NPP structural materials. *Yadern. Fiz. Atom. Energ.* **23**, 207 (2022) [in Ukrainian].
11. *Experimental Nuclear Reaction Data*. <https://www-nds.iaea.org/exfor/>.
12. R.A. Alvarez, B.L. Berman, D.D. Faul, F.H. Lewis Jr., P. Meyer. Photoneutron cross sections for  $^{55}\text{Mn}$  and  $^{59}\text{Co}$ . *Phys. Rev. C* **20**, 128 (1979).
13. R.A. Alvarez, B.L. Berman, P. Meyer. Photonuclear cross sections of  $^{58}\text{Ni}$  and  $^{60}\text{Ni}$ . *Phys. Rev. C* **10**, 608 (1974).
14. R.L. Bramblett, J.T. Caldwell, N.E. Hansen, C.P. Jupite. Photoneutron cross-sections for  $^{51}\text{V}$  and  $^{59}\text{Co}$ . *Phys. Rev.* **128**, 2345 (1962).
15. J. Kopecky. *Atlas of Neutron Capture Cross Sections* (JUKO Research, 1997).

Received 17.09.22.

Translated from Ukrainian by O.I. Voitenko

В.О. Желтонозський, Д.Є. Мизніков,

А.М. Саврасов, В.І. Слісенко

ВИЗНАЧЕННЯ ВМІСТУ  $^{59}\text{Ni}$  ТА  $^{55}\text{Fe}$

В КОНСТРУКЦІЙНИХ ЕЛЕМЕНТАХ АЕС

Проведено опромінювання конструкційних матеріалів 2-го блока ЧАЕС гальмівними  $\gamma$ -квантами з граничною енергією 37 МеВ. З виміряних  $\gamma$ -спектрів, використовуючи співвідношення виходів  $^{57}\text{Co}$ ,  $^{58}\text{Co}$  та  $^{54}\text{Mn}$ , ми визначили відношення концентрацій ізотопів  $^{58}\text{Ni}$  та  $^{56}\text{Fe}$  до концентрації  $^{59}\text{Co}$ . Із використанням отриманих даних та вимірної активності  $^{60}\text{Co}$  в досліджуваних зразках розроблено метод визначення активностей  $^{59}\text{Ni}$  та  $^{55}\text{Fe}$ . Проведено радіохімічну валідацію створеного методу і отримано гарне кількісне узгодження активностей  $^{59}\text{Ni}$  та  $^{55}\text{Fe}$ , знайдених спектроскопічним та радіохімічним методами.

Ключові слова: середньозважені виходи, фотоактиваційний метод, гамма-спектрометрія, нікель, залізо.